COMPARISON OF NONLINAR DYNAMIC RESPONSES OF EULER-BERNOULLI BEAMS AND TWO-DIMENSIONAL PLANE STRESS STATE OBTAINED FROM VEHICLE, IRREGULARITIES AND REINFORCED CONCRETE BRIDGE DYNAMIC INTERACTION SYSTEM

Thiago de Oliveira Abeche[1]

Roberto Dalledone Machado[2]

Ana Paula Imai[3]

Marcos Arndt[4]

t.abeche@gmail.com[1] / abeche@ufpr.br[1]

rdm@ufpr.br[2] / roberto.dalledonemachado@gmail.com[2]

ana_imai@hotmail.com[3]

arndt.marcos@gmail.com[4]

Numerical Methods in Engineering Graduate Program (PPGMNE), Concentration Area in Computational Mechanics, Federal University of Paraná (UFPR)[1,2,4]

Civil Construction Engineering Graduate Program (PPGECC), Concentration Area in Materials and Structures, Federal University of Paraná (UFPR)[2,3,4]

210 Cel. Francisco Heráclito dos Santos Street, 81531-990, Curitiba, Paraná, Brazil[1,2,3,4]

Abstract. *A numerical model is oftentimes considered representative if capable to approach the analytical solution with the least amount of error in the process. The measure of this approximation is an effective test for mathematical models by simulation of linear problems in well-known regimes or initial states of nonlinear problems. Several engineering problems, however, do not have an analytical solution. For these, in order to reach a consistent solution, it is necessary to consider some significant physical effects of the experiment. The damage mechanics and the plasticity theory are egregious sciences for representing the nonlinear dynamic diffuse cracking propagation on the concrete and the permanent deformations of the steel bars, respectively, in the dynamic interaction between vehicles, irregularities and reinforced concrete beams phenomena. These effects change the linear dynamic model into a nonlinear dynamic one with arduous convergence. Furthermore, a mathematical convergence not necessarily can represent a* *plausible physical solution. Moreover, the amount of nonlinear physical effects on the dynamic interaction systems can even make the problem more onerous, requiring greater computational efficiency, regarding both CPU time and memory requirements, and improved numerical methods. This works presents the theoretical foundations of the ABXDNL scientific research program developed with Euler-Bernoulli beam finite element, in order to compare the nonlinear dynamic responses with new proposed nonlinear dynamic model through two-dimensional plane stress nonlinear finite element theory. Additional routines in C++ programming language are developed to consider this new model. It is adopted a constitutive nonlinear dynamic damage model based on the Mazars' damage model, which also regards the effects of the inversion of mechanical solicitations due to vibrations. The structural damping is defined by the Rayleigh method with updated coefficients due to damage. The continuum damage mechanics is considered dynamically, requiring to evaluate the damage in each layer for each iteration within each time step. The equations of motion are obtained by nonlinear dynamic equilibrium and numerically integrated in time using the Newmark Method together with the Newton-Raphson iterative Method. This proposal seeks to contribute to the nonlinear dynamics research field, specifically to the study of health monitoring and structural integrity of damaged bridges structures.*

Keywords: *Nonlinear Dynamics, Damage Mechanics, Nonlinear Finite Element Method, Dynamic Interaction, Computational Mechanics*

1 INTRODUCTION

The emergence of new and complex structural systems, subjected to preponderantly dynamic actions is another important factor. This is the case, for example, of offshore structures, oil exploration and exploitation in the continental offshore. The dynamic analysis of these structures is fundamental because one of the most important loads to be considered in the project is due to wave action (Machado, 1983).

The problem of dynamic interaction between vehicles and bridges structures has been studied by researchers in the last 150 years. This problem is among the oldest problems of structural dynamics. Earlier on, analytical methods were applied to simple models varying the boundary conditions of problem. The development of computer and numerical methods such as the finite element method allowed complex and refined models to produce accurate results, which could be verified through experimental measurements (Beghetto & Abdalla Filho, 2010).

This paper seeks to present the theoretical foundations of ABXDNL scientific research program, in C++ programming language, previously developed to use nonlinear *Euler-Bernoulli* beam finite element and now improved to also use two-dimensional plane stress nonlinear finite element theory in order to analyse the nonlinear dynamic responses of a vehicle-irregularity-bridge dynamical system by damage mechanics and plasticity theory.

2 CONSTITUTIVE MODELS

This section presents the *Mazars*'s damage constitutive model for the concrete and plasticity constitutive model for the structural steel.

2.1 Mazars' damage constitutive model for the concrete

Rabotnov *et al.* (1970) proposed to consider the loss of material stiffness as a result of cracking. Posteriorly, the continuum damage mechanics was formalized based on thermodynamics of irreversible processes by Lemaitre & Chaboche (1985).

The damage evolution in the concrete is simulated with the damage constitutive model proposed by Mazars (1984). This model is based on some experimental evidences observed in uniaxial experiments in concrete, having the fundamental hypotheses (Pituba, 1998):

(a) the damage is represented by a scalar variable D $(0 \leq D \leq 1)$ whose evolution occurs when a reference value for the 'equivalent stretching' is exceeded;

(b) locally the damage comes from the existence of stretching deformations;

(c) its considered, that the damage is isotropic, although experimental tests show that the damage leads, in general, to an anisotropy of concrete, which may initially be considered as isotropic; and

(d) the damaged concrete behaves as an elastic medium, therefore the permanent deformation evidenced experimentally in a situation of unloading is neglected.

The extension state is locally characterized by a stretching or an equivalent strain, expressed as (Pituba, 1998)

$$\tilde{\varepsilon} = \sqrt{\langle \varepsilon_1 \rangle_+^2 + \langle \varepsilon_2 \rangle_+^2 + \langle \varepsilon_3 \rangle_+^2} \tag{1}$$

where ε_i are the principal strain components and its positive parts defined by

$$\langle \varepsilon_i \rangle_+ = \frac{1}{2}[\varepsilon_i + |\varepsilon_i|] = \begin{cases} \varepsilon_i & \text{, if } \varepsilon_i > 0 \\ 0 & \text{, otherwise} \end{cases} \tag{2}$$

It is adopted that the damage starts when the equivalent strain $\tilde{\varepsilon}$ reaches a value of the reference strain ε_{d0} determined in uniaxial tensile tests in correspondence to the maximum stress, as shown in Fig. 1.

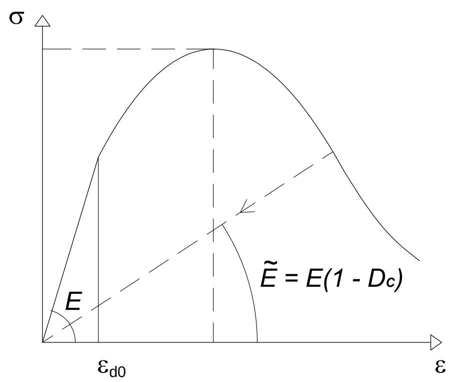

Figure 1: Compression stress-strain diagram for the Mazars' damage model

The constitutive relation, for the particular case of one-dimensional stress state, is given by

$$\sigma = (1 - D(\varepsilon))\, E_{c0}\varepsilon \tag{3}$$

In this model, when the equivalent deformation $\tilde{\varepsilon}$ reaches a certain limit value, ε_{d0} in this case, the damage evolution begins. This criterion can be written as a f function, as follows

$$f(\tilde{\varepsilon}, D) = \tilde{\varepsilon} - S(D) \leq 0, \quad S(0) = \varepsilon_{\text{d0}} \tag{4}$$

Admiting the continuity of the phenomena through time, the law of evolution of the damage variable that follows the principles of thermodynamics is defined by (Lemaitre & Chaboche, 1985)

$$\dot{D} = \begin{cases} 0 & \text{, if } f \leq 0 \text{ and } \dot{f} < 0 \\ F(\tilde{\varepsilon})\langle\dot{\tilde{\varepsilon}}\rangle_{+} & \text{, if } f = 0 \text{ and } \dot{f} = 0 \end{cases} \tag{5}$$

where $F(\tilde{\varepsilon})$ is a continuous and positive function of the equivalent deformation $\tilde{\varepsilon}$, such that $\dot{D} \geq 0$ for any $\dot{\tilde{\varepsilon}}$. This ensures that the damage is crescent and irreversible. In this sense, the $F(\tilde{\varepsilon})$ function must be capable to reproduce the observed experimental behavior in uni, bi and triaxial experiments.

Mazars (1984) defines two distinct damage variables, D_T and D_C representing, respectively, the tensile damage and compression damage. Thus, there are also two distinct laws of damage evolution

$$\dot{D}_T = F_T(\tilde{\varepsilon})\langle\dot{\tilde{\varepsilon}}\rangle_{+}, \qquad \dot{D}_C = F_C(\tilde{\varepsilon})\langle\dot{\tilde{\varepsilon}}\rangle_{+} \tag{6}$$

For cases where tensile and compressive stresses are simultaneously present in the stress states, the damage variable D is defined by a linear combination of the basic damage variables D_T and D_C through the combination coefficients α_T and α_C by

$$D(\varepsilon) = \alpha_T D_T + \alpha_C D_C, \qquad \alpha_T + \alpha_C = 1 \tag{7}$$

in which the value of the coefficients α_T and α_C are contained in the closed interval $[0, 1]$ and seek to represent the contribution of the mechanical requests to tensile and compression for the extension local state, respectively (Pituba & Proença, 2005).

This coefficients can be obtained by

$$\alpha_T = \frac{\Sigma_i\langle\varepsilon_{T_i}\rangle_{+}}{\varepsilon_V^{+}}, \qquad \alpha_C = \frac{\Sigma_i\langle\varepsilon_{C_i}\rangle_{+}}{\varepsilon_V^{+}} \tag{8}$$

where ε_{T_i} and ε_{C_i} are the deformation components determined by the positive and negative parts of the principal stress tensor obtained from the linear elastic constitutive relation.

Therefore, the deformations are defined as

$$\begin{cases} \{\varepsilon_T\} & = \frac{1+\nu}{E}\langle[\sigma]\rangle_+ - \frac{\nu}{E}\langle\Sigma_i\sigma_i\rangle_+ \,[I] \\ \{\varepsilon_C\} & = \frac{1+\nu}{E}\langle[\sigma]\rangle_- - \frac{\nu}{E}\langle\Sigma_i\sigma_i\rangle_- \,[I] \\ \varepsilon_V^+ & = \Sigma_i\langle\varepsilon_{T_i}\rangle_+ + \Sigma_i\langle\varepsilon_{C_i}\rangle_+ \end{cases} \tag{9}$$

where

$$\begin{cases} \langle\sigma_i\rangle_+ = \frac{1}{2}(\sigma_i + |\sigma_i|) \\ \langle\sigma_i\rangle_- = \frac{1}{2}(\sigma_i - |\sigma_i|) \end{cases} \tag{10}$$

The basic damage variables are given by (Mazars, 1984)

$$D_T(\tilde{\varepsilon}) = 1 - \frac{\varepsilon_{d0}\,(1 - A_T)}{\tilde{\varepsilon}} - \frac{A_T}{e^{B_T(\tilde{\varepsilon} - \varepsilon_{d0})}} \tag{11}$$

and

$$D_C(\tilde{\varepsilon}) = 1 - \frac{\varepsilon_{d0}\,(1 - A_C)}{\tilde{\varepsilon}} - \frac{A_C}{e^{B_C(\tilde{\varepsilon} - \varepsilon_{d0})}} \tag{12}$$

where A_T, B_T, A_C and B_T are the characteristic parameters of the material in uniaxial tensile and uniaxial compression, respectively, $\tilde{\varepsilon}$ the equivalent strain below which no damage occurs and ε_{d0} the parameter of the limit elastic deformation. The subscripts T and C refer to tensile and compression, respectively. Therefore, if the equivalent strain is lesser than the reference strain ($\tilde{\varepsilon} \leq \varepsilon_{\mathrm{d}0}$), then there is no damage at all $(D = 0)$.

In order to consider the Poisson effect in the concrete, the equivalent strain is given by

$$\tilde{\varepsilon} = \begin{cases} \varepsilon & \text{, if } \varepsilon \geq 0 \\ -\upsilon\sqrt{2\varepsilon} & \text{, otherwise} \end{cases} \tag{13}$$

where υ is the *Poisson's* ratio of the concrete.

Mazars (1984) proposed the following ranges of variation for the parameters A_T, B_T, A_C and B_T, obtained from the calibration with experimental results as (Pituba, 1998)

$$\begin{matrix} 0.7 \leq A_T \leq 1 & 10^4 \leq B_T \leq 10^5 & 10^{-5} \leq \varepsilon_{d0} \leq 10^{-4} \\ 1 \leq A_C \leq 1.5 & 10^3 \leq B_C \leq 2.10^3 & \end{matrix} \tag{14}$$

The behavior of the *Mazars'* damage model when the material is subjected to tensile is shown in the Fig. 2.

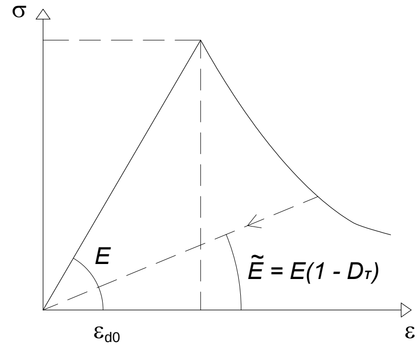

Figure 2: Tensile stress-strain diagram for the *Mazars'* damage model, adapted from (Pituba, 1998)

A more rigorous way to define the damage is through the fourth order damage tensor D_{ijrs} considering the operator that transforms the initial elasticity tensor of the intact material E_{ijkl} in the current elasticity tensor of the material softened by damage $\tilde{E}_{ijkl}$ by

$$\tilde{E}_{ijkl} = \left(I_{ijrs} - D_{ijrs}\right) E_{rskl} \tag{15}$$

From a purely theoretical point of view, the relationship shown above in Eq. (15) does not produce a true state variable because it requires knowledge of a particular behavior of the material, such as elasticity (Lemaitre & Desmorat, 2005). However, this relationship allows to indirectly determining the damage variable for elastic materials from Young's modulus measurements performed in tests with loading and unloading cycles.

In the case of uniaxial isotropic damage without the effect of micro cracks closure in compression, the average value of micro stresses is obtained from the equilibrium of forces (Rabotnov *et al.*, 1970). Thus, the effective stress can be written as

$$\tilde{\sigma} = \frac{F}{\tilde{S}} = \frac{F}{S(1-D)} = \frac{\sigma}{(1-D)} \tag{16}$$

where F is the applied force in the representative volume element, $\tilde{S}$ is the effective area which is the intact area S subtracted by the defects area S_D, and σ is the stress of the intact area.

Albeit this model neglects the permanent deformation in unloading situations, the damage is irreversible and cumulative. Therefore, if a damaged material has its load removed, the Young's modulus E is updated to the damaged Young's modulus $\tilde{E}$ and does not return to its initial state. It is only possible to cause more damage to the material, reducing the Young's modulus even more.

2.2 Plasticity constitutive model for the structural steel

A simple bilinear elastoplastic model with strain hardening is adopted for the structural steel as this material has the same behavior when subjected to tensile and compression. As in reinforced concrete structures the steel bars resist fundamentally the axial forces, it is used an uniaxial model to describe the behavior of the reinforcement.

Although very simplistic, the structural steel model is more reasonable than the linear elastic normative calculation models used in the majority of structural design offices for considering the hardening by plastic deformation. The Fig. 3 represents this model.

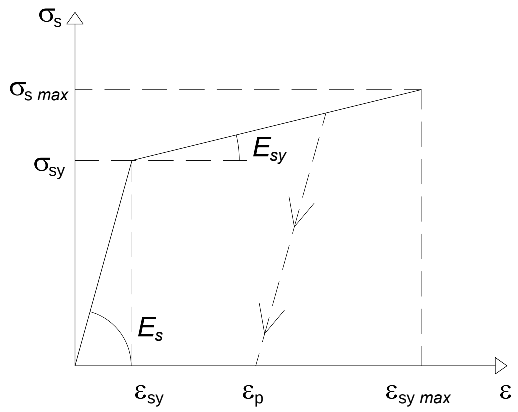

Figure 3: Bilinear elastoplastic model with strain hardening for the structural steel

where σ_{sy} is the yield stress, E_s is the initial Young modulus, ε_{sy} is the yield extension and E_{sy} is the elastic modulus after the yield of the steel bars.

The steel can suffer plasticity effect upon reaching the yield stress σ_{sy}. Therefore, the material will have a plastic strain ε_p within the ranges $+\varepsilon_{sy} \leq \varepsilon_p \leq +\varepsilon_{sy\ max}$ for a tensile case, or $-\varepsilon_{sy} \leq \varepsilon_p \leq -\varepsilon_{sy\ max}$ for a compression case. Thus, in this model, if the structural steel is unloaded at the second section of the diagram shown in Fig. 3, the model has a permanent strain, ε_p, associated.

In this plasticity constitutive model, the stress acting on the structural steel is determined by

$$|\sigma| = \begin{cases} |\sigma_{sy}| + E_{sy}(\varepsilon_p - |\varepsilon_{sy}|), & |\pm\varepsilon_{sy}| \leq \varepsilon_p \leq |\varepsilon_{sy\,max}| \\ E_s|\varepsilon_{sy}|, & -\varepsilon_{sy} \leq \varepsilon_{el} \leq \varepsilon_{sy} \end{cases} \tag{17}$$

where ε_{el} is the linear elastic strain.

3 BRIDGE STRUCTURE MODELS THROUGH NONLINEAR FINITE ELEMENT METHOD

This section presents two diffent models for the bridge structure: one modelled through two-dimensional plane stress state and other through *Euler-Bernoulli* beam.

3.1 Two-dimensional plane stress state

Firstly, it is adopted the quadrilateral two-dimensional plane stress linear finite element with 4 nodes, with L_1 and L_2 dimensions, as shown below.

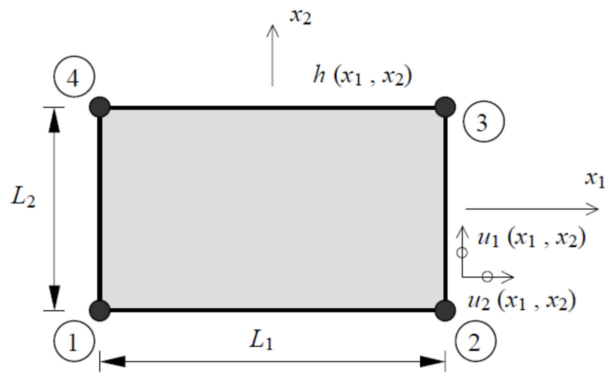

Figure 4: Two-dimensional plane stress linear finite element with 4 nodes (Bathe, 1996)

The shape functions for this type of element with L_1 and L_2 dimensions are

$$\begin{cases} N_1\left(x_1, x_2\right) = \frac{1}{L_1 L_2}\left(\frac{L_1}{2} - x_1\right)\left(\frac{L_2}{2} - x_2\right) \\ N_2\left(x_1, x_2\right) = \frac{1}{L_1 L_2}\left(\frac{L_1}{2} + x_1\right)\left(\frac{L_2}{2} - x_2\right) \\ N_3\left(x_1, x_2\right) = \frac{1}{L_1 L_2}\left(\frac{L_1}{2} + x_1\right)\left(\frac{L_2}{2} + x_2\right) \\ N_4\left(x_1, x_2\right) = \frac{1}{L_1 L_2}\left(\frac{L_1}{2} - x_1\right)\left(\frac{L_2}{2} + x_2\right) \end{cases} \tag{18}$$

By expanding the N_i functions, it can be noted that the shape functions miss the quadratic terms of second degree. In this sense, the shape functions N_i are incomplete second degree polynomials. This will be further discussed due its influence on the nonlinear responses, especially in the nonlinear dynamic ones.

The finite element stiffness matrix of two-dimensional plane stress state is defined by

$$[K] = \int_\Omega [B]^T[D][B]\mathrm{d}\Omega = \int_S [B]^T[D][B]h\mathrm{d}S = \int_{\frac{-L_2}{2}}^{\frac{L_2}{2}} \int_{\frac{-L_1}{2}}^{\frac{L_1}{2}} [B]^T[D][B]h\mathrm{d}x_1\mathrm{d}x_2 \tag{19}$$

The finite element mass matrix, on other hand, can be defined by

$$[m] = \int_\Omega \rho[N]^T[N]\mathrm{d}\Omega \tag{20}$$

The relation between stress and strain tensors for isotropic materials in a plane stress state is defined by

$$[\sigma] = [D][\varepsilon] \tag{21}$$

where σ, D and ε represent, respectively, the stress, the elasticity and the strain tensors.

The Eq. (21) can be expanded as

$$\begin{Bmatrix} \sigma_1 \\ \sigma_2 \\ \sigma_3 \end{Bmatrix} = \frac{E}{1-\upsilon^2} \begin{bmatrix} 1 & \upsilon & 0 \\ \upsilon & 1 & 0 \\ 0 & 0 & \frac{1-\upsilon}{2} \end{bmatrix} \begin{Bmatrix} \varepsilon_1 \\ \varepsilon_2 \\ \gamma_{12} \end{Bmatrix} \tag{22}$$

In order to consider the physical nonlinear phenomena in the analysis, it is of the utmost importance to calculate the variables in the *Gaussian* points. To make this possible, it is necessary to develop a general quadrilateral finite element with an arbitrary geometry.

The integrals, in these cases, need to be calculated in an irregular quadrilateral integration domain defined by the element nodes. To simplify the proccess and aiming to calculate the integrals at the *Gaussian* points, it is greatly advantageous to replace the variables x_1 and x_2, as follows

$$\begin{cases} x_1 \rightarrow x_1(s_1, s_2) \\ x_2 \rightarrow x_2(s_1, s_2) \end{cases} \tag{23}$$

with the integration limit in both directions defined by the interval $[-1, 1]$.

The change of the coordinate system is performed by interpolation. Thus, the shape fuctions are easily obtained by substituting x_i by s_i in Eq. (18), as shown below

$$\begin{cases} N_1\left(s_1, s_2\right) = \frac{1}{4}\left(1-s_1\right)\left(1-s_2\right) \\ N_2\left(s_1, s_2\right) = \frac{1}{4}\left(1+s_1\right)\left(1-s_2\right) \\ N_3\left(s_1, s_2\right) = \frac{1}{4}\left(1+s_1\right)\left(1+s_2\right) \\ N_4\left(s_1, s_2\right) = \frac{1}{4}\left(1-s_1\right)\left(1+s_2\right) \end{cases} \tag{24}$$

After replacing the variables, the stiffness matrix becomes

$$[K] = \int_{-1}^{1}\int_{-1}^{1} [B]^T [D][B] h \|J\| \mathrm{d}s_1 \mathrm{d}s_2 \tag{25}$$

where $\|J\|$ is the determinant of the *Jacobian* matrix, or transformation matrix, defined by

$$[J] = \begin{bmatrix} \frac{\partial x_1}{\partial s_1} & \frac{\partial x_1}{\partial s_2} \\ \frac{\partial x_2}{\partial s_1} & \frac{\partial x_1}{\partial s_2} \end{bmatrix} \tag{26}$$

The components of the *Jacobian* matrix can be obtained through matrix multiplication of the cartesian coordinates as follows

$$[J] = \begin{bmatrix} \frac{\partial x_1}{\partial s_1} & \frac{\partial x_1}{\partial s_2} \\ \frac{\partial x_2}{\partial s_1} & \frac{\partial x_1}{\partial s_2} \end{bmatrix} = \begin{bmatrix} x_{11} & x_{21} & x_{31} & x_{41} \\ x_{12} & x_{22} & x_{32} & x_{42} \end{bmatrix} \begin{bmatrix} \frac{\partial N_1}{\partial s_1} & \frac{\partial N_1}{\partial s_2} \\ \frac{\partial N_2}{\partial s_1} & \frac{\partial N_2}{\partial s_2} \\ \frac{\partial N_3}{\partial s_1} & \frac{\partial N_3}{\partial s_2} \\ \frac{\partial N_4}{\partial s_1} & \frac{\partial N_4}{\partial s_2} \end{bmatrix} \tag{27}$$

where the rightmost matrix, $\left[\frac{\partial N}{\partial s}\right]$, is simple obtained by deriving the shape functions N_i in relation to s_i.

The deformation tensor for the element utilized in this section is defined by

$$[B] = \begin{bmatrix} \frac{\partial N_1}{\partial x_1} & 0 & \frac{\partial N_2}{\partial x_1} & 0 & \frac{\partial N_3}{\partial x_1} & 0 & \frac{\partial N_4}{\partial x_1} & 0 \\ 0 & \frac{\partial N_1}{\partial x_2} & 0 & \frac{\partial N_2}{\partial x_2} & 0 & \frac{\partial N_3}{\partial x_2} & 0 & \frac{\partial N_4}{\partial x_2} \\ \frac{\partial N_1}{\partial x_2} & \frac{\partial N_1}{\partial x_1} & \frac{\partial N_2}{\partial x_2} & \frac{\partial N_2}{\partial x_1} & \frac{\partial N_3}{\partial x_2} & \frac{\partial N_3}{\partial x_1} & \frac{\partial N_4}{\partial x_2} & \frac{\partial N_4}{\partial x_1} \end{bmatrix} \tag{28}$$

In order to obtain the necessary components of the tensor, the subsequent operation can be performed

$$\begin{bmatrix} \frac{\partial N_1}{\partial x_1} & \frac{\partial N_1}{\partial x_2} \\ \frac{\partial N_2}{\partial x_1} & \frac{\partial N_2}{\partial x_2} \\ \frac{\partial N_3}{\partial x_1} & \frac{\partial N_3}{\partial x_2} \\ \frac{\partial N_4}{\partial x_1} & \frac{\partial N_4}{\partial x_2} \end{bmatrix} = \begin{bmatrix} \frac{\partial N_1}{\partial s_1} & \frac{\partial N_1}{\partial s_2} \\ \frac{\partial N_2}{\partial s_1} & \frac{\partial N_2}{\partial s_2} \\ \frac{\partial N_3}{\partial s_1} & \frac{\partial N_3}{\partial s_2} \\ \frac{\partial N_4}{\partial s_1} & \frac{\partial N_4}{\partial s_2} \end{bmatrix} \begin{bmatrix} \frac{\partial x_1}{\partial s_1} & \frac{\partial x_1}{\partial s_2} \\ \frac{\partial x_2}{\partial s_1} & \frac{\partial x_1}{\partial s_2} \end{bmatrix}^{-1} \tag{29}$$

Finally, the obtained components are reallocated in the deformation tensor $[B]$.

A multiple integral whose limits of integration are defined by the interval $[-1, 1]$ for all the variables can be calculated by the *Gaussian* quadrature. For the bidimensional case

$$\int_{-1}^{1}\int_{-1}^{1} f(s_1, s_2)\mathrm{d}s_1\mathrm{d}s_2 \cong \sum_{l=1}^{n_{p1}}\sum_{m=1}^{n_{p2}} W_l W_m f(P_l, P_m) \tag{30}$$

where n_{p1} and n_{p2} are the *Gaussian* points associated with directions s_1 and s_2, respectively. Analogously, W_l and W_m are the weights associated with their directions.

By replacing Eq. (25) in Eq. (30), one can obtain

$$f(s_1, s_2) = f(P_l, P_m) = [B]^T[D][B]h\|J\| \tag{31}$$

Therefore, the stiffness matrix can be calculated at any point of any element. Similarly, after obtaining the dynamic responses of displacement, velocity and acceleration by solving the equation of motion, it is also possible to evaluate the stress and deformation states. Nonetheless, it is found that there is much greater precision if the selected points coincide with the corresponding *Gaussian* points. For evaluation of the structure by the damage machanics, this procedure is essential in order to achieve convergence and mathematical responses consistent with the actual physical responses of the structure.

3.2 Euler-Bernoulli beam

The shape functions for the *Euler-Bernoulli* element are *Hermitian* cubic interpolation functions, defined as

$$\begin{cases} H_1(x_1) = \frac{1}{2} - \frac{3x_1}{2L} + \frac{2x_1^3}{L^3} \\ H_2(x_1) = \frac{L}{8} - \frac{x_1}{4} - \frac{x_1^2}{2L} + \frac{x_1^3}{L^2} \\ H_3(x_1) = \frac{1}{2} + \frac{3x_1}{2L} - \frac{2x_1^3}{L^3} \\ H_4(x_1) = -\frac{L}{8} - \frac{x_1}{4} + \frac{x_1^2}{2L} + \frac{x_1^3}{L^2} \end{cases} \tag{32}$$

From the principle of virtual works, for example, one can obtain

$$\begin{aligned} [K] &= \int_\Omega [B]^T [D][B] \mathrm{d}\Omega = \\ &= \int_{\frac{-L}{2}}^{\frac{L}{2}} \{B\}^T \{B\} E \int_S x_3^2 \mathrm{d}S \mathrm{d}x_1 = EI_2 \int_{\frac{-L}{2}}^{\frac{L}{2}} \{B\}^T \{B\} \mathrm{d}x_1 \end{aligned} \tag{33}$$

The transformation now correspond to the first term in Eq. (23). The substitution of the coordinate x_1 for the coordinate s_1 is simple made with $x_1 = \frac{L}{2}s_1$. In this case, the *Jacobian* is a scalar defined by $J = \frac{\mathrm{d}x_1}{\mathrm{d}s_1} = \frac{L}{2}$. Thus, the shape functions are defined by

$$\begin{cases} H_1(s_1) = \frac{1}{2} - \frac{3s_1}{4} + \frac{s_1^3}{4} \\ H_2(s_1)\,J = \left(\frac{1}{4} - \frac{s_1}{4} - \frac{s_1^2}{4} + \frac{s_1^3}{4}\right) J \\ H_3(s_1) = \frac{1}{2} + \frac{3s_1}{4} - \frac{s_1^3}{4} \\ H_4(s_1)\,J = \left(-\frac{1}{4} - \frac{s_1}{4} + \frac{s_1^2}{4} + \frac{s_1^3}{4}\right) J \end{cases} \tag{34}$$

In order to calculate the components of the deformation tensor $\{B\}$, the follow operations may be performed, according to the chain rule

$$\begin{aligned} &\frac{\mathrm{d}H_i}{\mathrm{d}s_1} = \frac{\mathrm{d}H_i}{\mathrm{d}x_1}\frac{\mathrm{d}x_1}{\mathrm{d}s_1} \rightarrow \frac{\mathrm{d}}{\mathrm{d}s_1}\left(\frac{\mathrm{d}H_i}{\mathrm{d}s_1}\right) = \frac{\mathrm{d}}{\mathrm{d}x_1}\left(\frac{\mathrm{d}H_i}{\mathrm{d}s_1}\right)\frac{\mathrm{d}x_1}{\mathrm{d}s_1} \rightarrow \frac{\mathrm{d}^2 H_i}{\mathrm{d}s_1^2} = \frac{\mathrm{d}}{\mathrm{d}x_1}\left(\frac{\mathrm{d}H_i}{\mathrm{d}x_1}J\right)J \\ &\frac{\mathrm{d}^2 H_i}{\mathrm{d}x_1^2} = \frac{\mathrm{d}^2 H_i}{\mathrm{d}s_1^2}\frac{1}{J^2} \end{aligned} \tag{35}$$

Therefore, the deformation tensor $\{B\}$ is obtained by

$$\{B\} = \left\{ -\frac{\mathrm{d}^2 H_1}{\mathrm{d}x_1^2} \quad -\frac{\mathrm{d}^2 H_2}{\mathrm{d}x_1^2} \quad -\frac{\mathrm{d}^2 H_3}{\mathrm{d}x_1^2} \quad -\frac{\mathrm{d}^2 H_4}{\mathrm{d}x_1^2} \right\} = \left\{ -\frac{6s_1}{L^2} \quad \frac{1}{L} - \frac{3s_1}{L} \quad \frac{6s_1}{L^2} \quad -\frac{1}{L} - \frac{3s_1}{L} \right\} \tag{36}$$

Thus, the Eq. (33) becomes

$$[K] = EI_2 \int_{-1}^{1} \{B\}^T \{B\} \frac{\mathrm{d}x_1}{\mathrm{d}s_1} \mathrm{d}s_1 = EI_2 \sum_{l=1}^{n_{p1}} W_l f(P_l), \quad f(s_1) = f(P_l) = \{B\}^T \{B\} J \tag{37}$$

Equivalent stiffness model

To be able to simulate the damage mechanics in *Euler-Bernoulli* beam finite elements, the consideration of other dimensions, x_2 and x_3, for the geometry and material properties are required. The rectangular cross section of the bridge's elements are divided in n layers as laminated composite beams in order to be able to determine the equivalent stiffness of each element. The Fig. 5 shows this division.

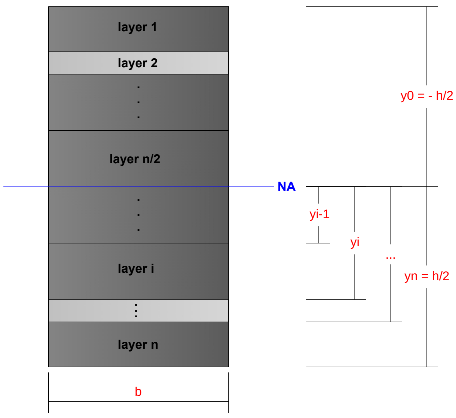

Figure 5: *Euler-Bernoulli* beam cross-section divided in n layers

For the particular case of symmetric laminated composite beam with b width, the equivalent stiffness EI_{eqv} is determined by

$$EI_{eqv} = \frac{1}{3} \sum_{i=1}^{n} E_i (y_i^3 - y_{i-1}^3) \tag{38}$$

where n is the number of layers, b is the constant width of the rectangular cross section, E_i is the elastic modulus of the i^{th} layer, in the case E_c for the concrete layers and E_s for the structural steel layers, y_i and y_{i-1} are the y axis coordinate values of the i^{th} division points which subtracted result in the height of the layer.

When the concrete or structural steel, present nonlinear physical behavior, the position of the neutral axis varies and is recalculated at each numerical iteration according to the deterioration or plastification of any layer by

$$y_{\text{NA}} = \frac{\sum \left(\frac{y_i - y_{i-1}}{2}\right) E_i A_i}{\sum E_i A_i} \tag{39}$$

in which A_i is the area of the layer and y_{NA} is the recalculated position of the neutral axis.

As the continuum damage mechanics is calculated dynamically, in order to consider these effects, it is required to evaluate the damage in each cross section of the bridge's elements for each iteration within each time steps. When considering this variation, it is possible to capture the stress invesion due, among other reasons, to vibrations.

4 COMPUTATIONAL MODEL FOR THE DYNAMIC INTERACTION BETWEEN THE SYSTEMS

4.1 Linear dynamic mathematical model

Just to describe the linear case in order to understand the nonlinear dynamic mathematical model, this subsection will simple describes a few particularities of the linear model and its governing equation.

Differently from the nonlinear dynamic model, on the linear one no distinctions are made for the elastic tensor $[D]$. On finite element two-dimensional plane stress state, the *Young's* modulus and the *Poisson's* ratio remain constant through all the analysis. On the *Euler-Bernoulli's* beam finite element, additionally, there is no consideration of the cross-sectional geometry. Thus, only the moment of inertia and the *Young's* modulus are taken in consideration, both of them constants through time.

The governing equation of this problem is shown in Eq. (40)

$$[m]\{\ddot{u}\} + [C]\{\dot{u}\} + [K]\{u\} = \{F(t)\} \tag{40}$$

where $[m]$, $[C]$ and $[K]$ are the global matrices of mass, damping and stiffness, $\{\ddot{u}\}$, $\{\ddot{u}\}$ and $\{u\}$ are the global vectors of displacements, velocities and accelerations and, finally, the $\{F(t)\}$ represents the external force vector that varies over time.

To solve the Eq. (40), one may use a time integration method, such as the *Newmark* method. The system, after that, can be solved by the *Gaussian* elimination method in each time step.

4.2 Nonlinear dynamic mathematical model by damage mechanics

In a case of deterioration of the material, the forces are no longer linearly dependent of the displacements. This model considers that the damage directly affects the stiffness of the system and consequently the structural damping but not the mass of the system, as a case of a rocket launch, thus causing the previously fixed stiffness matrix to become instantaneous, characterizing physical nonlinearity, as shown below (Abeche *et al.*, 2015)

$$[K_B] = [K_B\left(\{u_B(\vec{x}, t)\}\right)] \tag{41}$$

It can be noted that the previously fixed stiffness matrix is now instantaneous. It is dependent of the displacements which are a functional of time and position vector. Thus, the predictive values, or estimates, of velocities and displacements in time t with respect to time $t+\Delta t$ are respectively defined as (Machado, 1983)

$$\begin{cases} \{\tilde{\dot{u}}_B\}_{t+\Delta t} = \{\dot{u}_B\}_t + (1-\gamma)\{\ddot{u}_B\}_t\Delta t \\ \{\tilde{u}_B\}_{t+\Delta t} = \{u_B\}_t + \{\dot{u}_B\}_t\Delta t + \left(\frac{1}{2}-\beta\right)\{\ddot{u}_B\}_t\Delta t^2 \end{cases} \tag{42}$$

where γ and β are the *Newmark* method parameters determined for the numerical integration accuracy and stability.

Due to physical nonlinearities, the previous linear global equation of motion presented in Eq. (43) becomes nonlinear dynamic and must be solved iteratively and incrementally by combining the iterative *Newton-Raphson* technique with the implicit time integration operator of the *Newmark* method. In this sense, the nonlinear dynamic global equation of motion for the damaged highway bridge can be written as (Jacob & Ebecken, 1994)

$$[M_B]^{(i-1)}_{t+\Delta t}\{\ddot{u}_B\}^{(i)}_{t+\Delta t} + [C_B]^{(i-1)}_{t+\Delta t}\{\dot{u}_B\}^{(i)}_{t+\Delta t} + [K_B]^{(i-1)}_{t+\Delta t}\{\Delta u\}^{(i)} = \{\Delta F_B\} \tag{43}$$

where

$$\{\Delta F_B\} = \{F_B^{ext}\}_{t+\Delta t} - \{F_B^{int}\}^{(i-1)}_{t+\Delta t} \tag{44}$$

and where i is the present iteration, $\{F_B^{ext}\}_{t+\Delta t}$, $\{F_B^{int}\}_{t+\Delta t}$ and $\{\Delta F_B\}_{t+\Delta t}$ are, respectively, the external forces vector, the internal forces vector and the unbalanced forces vector in time $t+\Delta t$ and $\{\Delta u\}$ is the incremental displacements vector.

It can be observed that by combining the *Newton-Raphson* iterative technique with the Newmark method and the predictive values, the internal forces seeks the nonlinear dynamic equilibrium in each iteration within each time step in order to make the unbalanced forces vector tend to null vector with respect to a convergence criterion.

Applying Eq. (42) in Eq. (43), one obtains (Abeche *et al.*, 2016)

$$\begin{aligned} &\left(\frac{[M_B]^{(i-1)}_{t+\Delta t}}{\beta\Delta t^2} + \frac{\gamma[C_B]^{(i-1)}_{t+\Delta t}}{\beta\Delta t}\right)\{u_B\}^{(i)}_{t+\Delta t} + [K_B]^{(i-1)}_{t+\Delta t}\{\Delta u\}^{(i)} = \\ &\{F_B^{\text{ext}}\}_{t+\Delta t} + \frac{[M_B]^{(i-1)}_{t+\Delta t}}{\beta\Delta t^2}\left(\{u_B\}_t + \{\dot{u}_B\}_t\Delta t + \left(\frac{1}{2}-\beta\right)\{\ddot{u}_B\}_t\Delta t^2\right)^{(i)} \\ &+ [C_B]^{(i-1)}_{t+\Delta t}\left(\frac{\gamma}{\beta\Delta t} + \left(\frac{\gamma}{\beta}-1\right)\{\dot{u}_B\}_t + \left(\frac{\gamma}{2\beta}-1\right)\{\ddot{u}_B\}_t\Delta t\right)^{(i)} - \{F_B^{\text{int}}\}^{(i-1)}_{t+\Delta t} \end{aligned} \tag{45}$$

The damping matrix becomes nonlinear and dynamic, as defined in Eq. (46).

$$[C_B(\{u_B(\overrightarrow{x},t)\})]^{(i-1)}_{t+\Delta t} = (\tilde{\alpha}_B)^{(i-1)}_{t+\Delta t}[M_B]^{(i-1)}_{t+\Delta t} + (\tilde{\beta}_B)^{(i-1)}_{t+\Delta t}[K_B(\{u_B(\overrightarrow{x},t)\})]^{(i-1)}_{t+\Delta t} \tag{46}$$

The internal global force seeks the nonlinear dynamic equilibrium configuration. Its components are the forces parcels from the stresses acting in each of the layers of the cross section for each element. These are obtained at each iteration within each time step as (Bathe, 1996)

$$\{F_B^{int}\}_{t+\Delta t}^{(i-1)} = \sum_m \int_{V_{t+\Delta t}^{(m)}} [B]_{t+\Delta t}^{(m)^T} [\sigma]_{t+\Delta t}^{(m)} \mathrm{d}V_{t+\Delta t}^{(m)} \tag{47}$$

Making use of the *Gaussian* quadrature technique, the internal global force seeks the nonlinear dynamic equilibrium configuration in each iteration of the iterative *Newton-Raphson* technique, within each time step of the *Newmark* method.

The convergence criteria utilized is related to an energy criteria that includes both forces and displacements criteria, defined as (Bathe, 1996)

$$\{\Delta u\}^{(i)^T} \left(\{F_B^{ext}\}_{t+\Delta t} - \{F_B^{int}\}_{t+\Delta t}^{(i-1)}\right) \le tol_E \left(\{\Delta u\}^{(1)^T} \left(\{F_B^{ext}\}_{t+\Delta t} - \{F_B^{int}\}_t\right)\right) \tag{48}$$

where tol_E is the energy convergence tolerance.

After obtaining the nonlinear dynamic responses at the end of the iteration within the required time step, a further time step is started whenever one wishes to calculate the dynamic displacements, velocities, accelerations, etc., for a new time period, until the last time of the analysis is reached, in which the process is terminated.

The ABXDNL 2.9 program was developed for solving the nonlinear dynamic Eq. (45), considering the damage mechanics and plasticity theory within *Euler-Bernoulli* and two-dimensional plane stress finite elements.

5 NUMERICAL ANALYSIS AND CONCLUSIONS

This paper seeks to compare the dynamic responses, influenced by damage mechanics and plasticity theory, of *Euler-Bernoulli* and two-dimensional plane stress finite elements. The Tables 1 and 2 present the input data for the simulations.

Table 1: Bridge's parameters input data

Euler-Bernoulli	Two-dimensional plane stress	Materials	Geometric
20 Elements	240 Elements	$E_c = 29.43$ GPa	$b = 1$ m
-	20 x-Elements	$\nu_c = 0.2$	$h = 4$ m
-	12 y-Elements	10 Concrete's Layers	$I_b = 5.\bar{3}$ m^4
2 dof / element	2 dof / element	$E_s = 210$ GPa	12 Layers
$2\ \frac{\text{nodes}}{\text{element}}$	$4\ \frac{\text{nodes}}{\text{element}}$	$\nu_s = 0.3$	$A_c = 3.96$ m^2
2 boundary conditions	3 boundary conditions	2 Steel's Layers	$A_s = 0.06$ m^2
$\text{L}_\text{e} = 1$ m	$\text{L}_1 = 1$ m	$\rho_s = 7800$ kg/m^3	$d = 3.77$ m
-	$\text{L}_2 =$ variable	$\rho_c = 2400$ kg/m^3	$d' = 0.23$ m
$m = \frac{\text{variable}}{\text{element's layer}}$	$m = \frac{\text{variable}}{\text{element}}$	$\rho = 1.52284264\%$	$L_b = 20$ m

Table 2: Vehicle-irregularities coupled model, dynamical and damage parameters input data

Vehicle	Irregularities	Dynamical	Damage Parameters
$m_1 = 4400$ kgf	$y = A\sin(\omega_e t)$	$\gamma = 0.5$	$A_T = 0.995$
$m_2 = 17600$ kgf	$l = 1$ m	$\beta = 0.25$	$B_T = 30000$
$k = 9120$ kN/m	$A = 0.005$ m	$dt = 7.2\ \mathrm{e}^{-4}$ s	$A_C = 1.2$
$c = 86$ kNs/m	$\omega_e = 87.2665$ rad/s	3000 Time Steps	$B_C = 1050$
$v = 50$ km/h	-	$\zeta = 0.025$	$\varepsilon_{\mathrm{d0}} = 5\mathrm{e}^{-5}$
$a = 0$ m/s^2	-	$tol_u = 0.00001$	-
2000 Time Steps	2000 Time Steps	$tol_F = 0.00001$	-
-	-	$tol_E = 0.00001$	-

The boundary conditions adopted restrict the *Euler-Bernoulli*'s vertical displacement degrees of freedom in both extremities. The boundary conditions for the plane-stress, otherwise, restrict the vertical and horizontal displacements at the left extremity and the vertical one at the the right end for the elements located on the central axis. The mesh utilized in both models, being the equivalent stiffness for *Euler-Bernoulli*, is presented in Fig. 6.

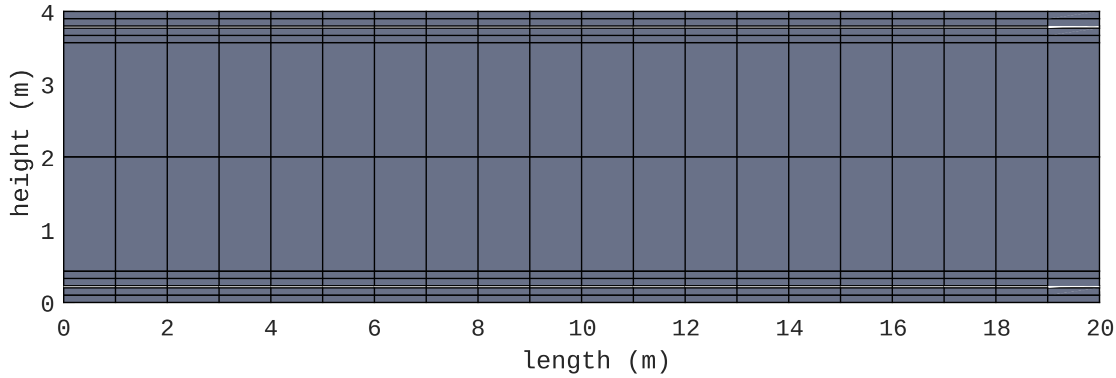

Figure 6: Mesh utilized in *Euler-Bernoulli* and Plane Stress nonlinear dynamic models

The Table 3 shows the reduction of the first natural frequency of vibration obtained in both models.

Table 3: Reduction of the natural frequencies of vibration for both models

Natural frequencies	*Euler-Bernoulli*		Plane Stress State	
of vibration	Linear	Nonlinear	Linear	Nonlinear
1$^{\mathrm{st}}$	108.3987335	93.8970054	102.4768100	85.9663032

Obviously, one can note the difference in linear responses due to the difference in the degrees of freedom of the models. The dynamic damage effect reduced the natural frequencies on the nonlinear results. The reduction were more drastic in the plane stress FE model.

The Fig. 7 illustrates the final damaged configuration for both plane stress and *Euler-Bernoulli* finite element models that caused the stiffness reduction for all the nonlinear results.

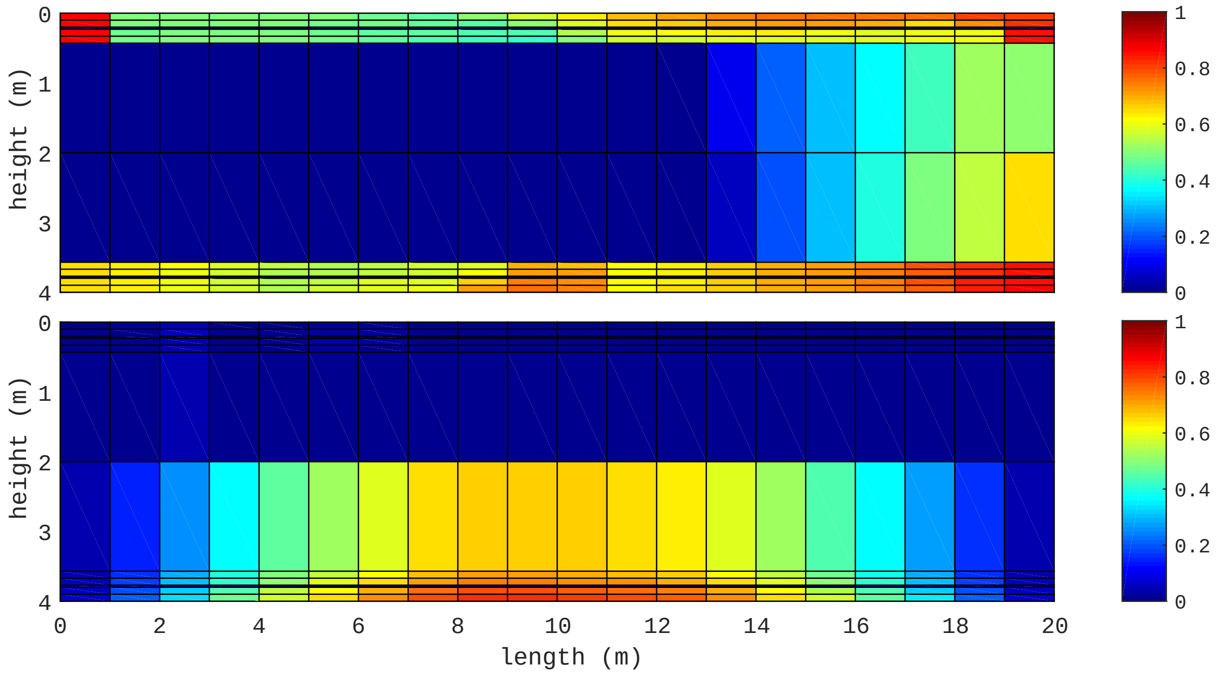

Figure 7: Final damaged configuration for: (a) Plane Stress State FEM, (b) *Euler-Bernoulli* FEM

The dynamic responses of acceleration for both models are shown in Fig. 8.

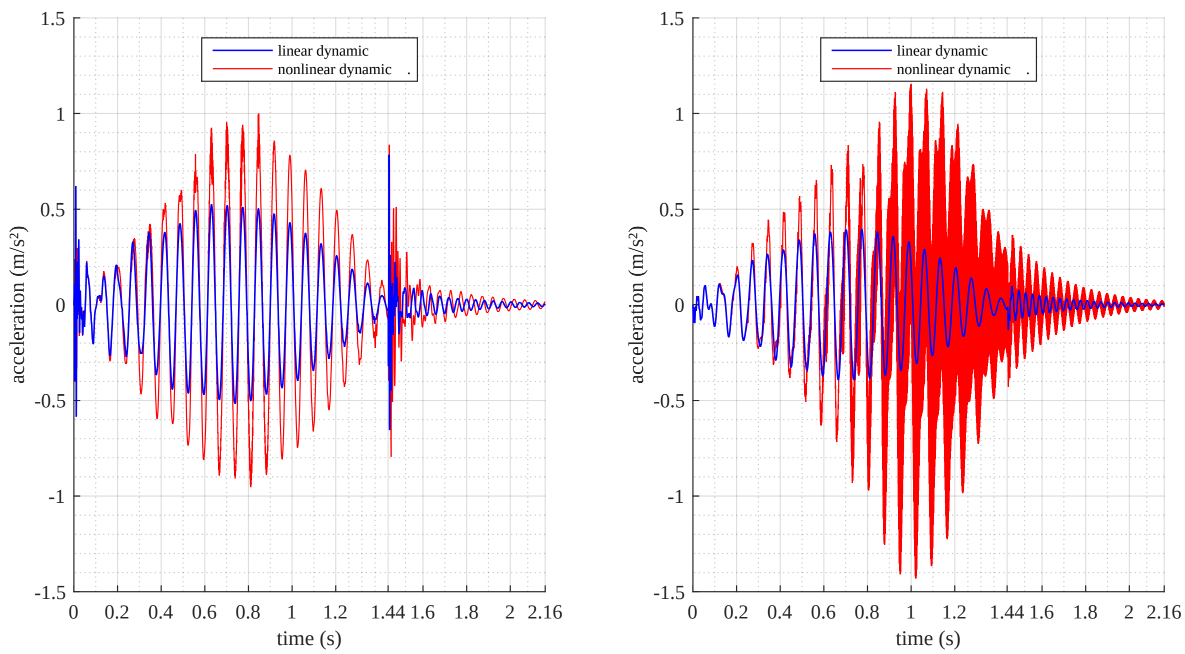

Figure 8: Dynamic responses of acceleration obtained from: (a) PSS midspan, (b) *Euler-Bernoulli* midspan

Clearly, there were acceleration peaks for the nonlinear dynamic responses obtained from both models. This could justify the difference between the experimental responses obtained through accelerometers with the responses of computational simulations obtained through linear dynamic models. The amplification difference in both models responses occurred not only due to the difference in the dynamic damage evolution observed in Fig. 7 but also by the physical representation involved in them, as can be observed in the linear dynamic responses.

The Fig. 9 shows the static, linear and nonlinear dynamic responses of vertical displacement obtained from the lower and central degree of freedom of plane stress model and from the central one in *Euler-Bernoulli* model.

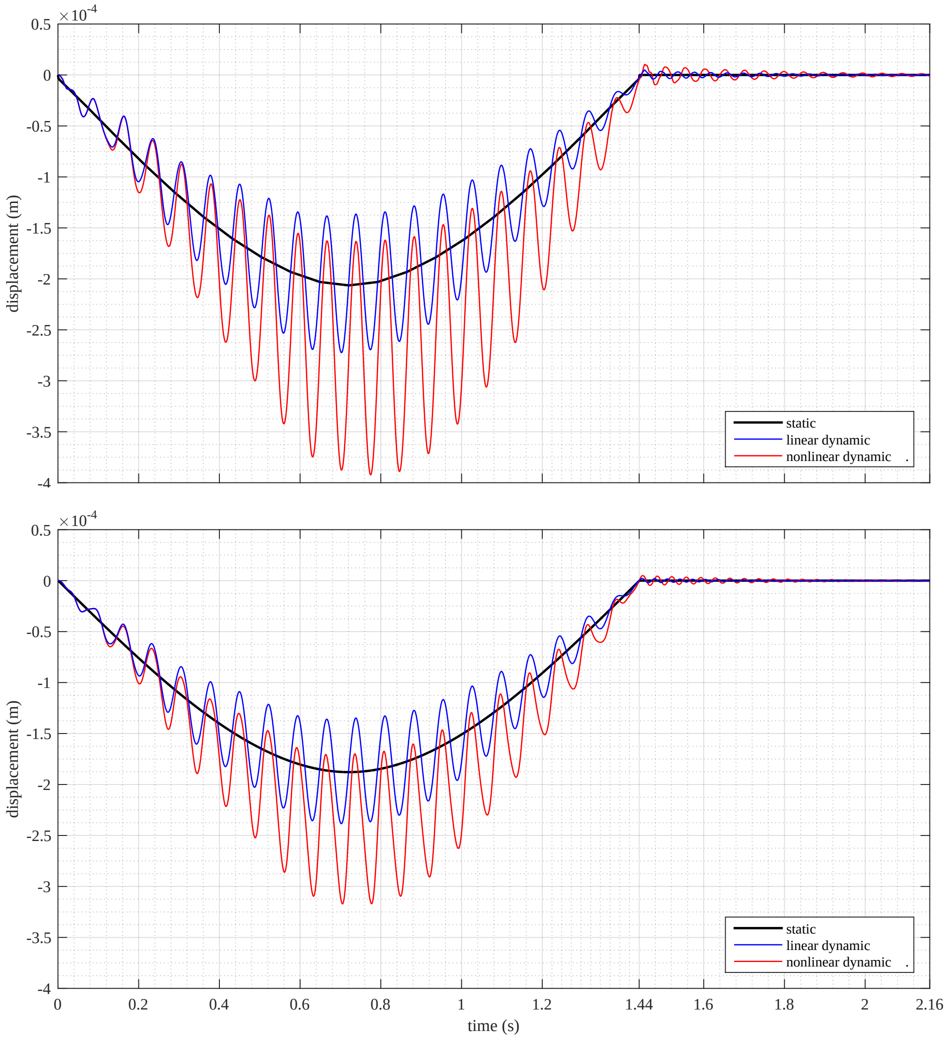

Figure 9: Dynamic responses of displacement obtained from: (a) PSS midspan, (b) *Euler-Bernoulli* midspan

It can be observed that the linear dynamic ones oscillates around the static responses through time. The nonlinear dynamic responses obtained from both systems were amplified by damage mechanics. During the vehicle's movement on the bridge, there were no increase in the frequency of dynamic responses. This is a typical behavior of nonlinear dynamic responses by damage mechanics from sinusoidal harmonic excitations while there is not a complete failure of the material.

The responses were obviously greater from the plane stress model, both linear and nonlinear ones. This is inherent to the characteristic of the models: in *Euler-Bernoulli* FEM a bar is moving accordling only to vertical displacements and rotations from its degrees of freedom, without considering the horizontal displacements, even when incorporating the equivalent stiffness model, while in plane stress FEM the responses are due only to vertical and horizontal displacements of a two-dimensional element, without the rotation.

Still, it is also noted that nonlinear dynamic responses were greater in the plane stress model. Thus, the dynamic damage evolution were increased in this model. This can be occasioned by stress concentration in two-dimensional problems and, especially, due to the shape functions of this element. The fact that these functions miss the quadratic terms of a second degree polynomial, being an incomplete polynomial function, directly affects the nonlinear behavior. If in linear problems, even in static one, this is an issue of utmost importance, in nonlinear problems, especially in dynamics, this complete affects the responses since a refinement with this incomplete functions will not necessarily assure consistent responses.

In any case, in this study, no results are presented with mesh refinement, since this type of analysis is not the focus of the present paper. However, although with the unimproved mesh utilized in this work, approached linear responses for both models were obtained, further mesh refinement could lead to some gain in nonlinear response. But, with better shape functions of more complex elements a minor refinement could greatly improve nonlinear responses.

The dynamic responses of velocity obtained from both models are presented as shown in Fig. 10. All conclusions discussed above can be observed in the responses below.

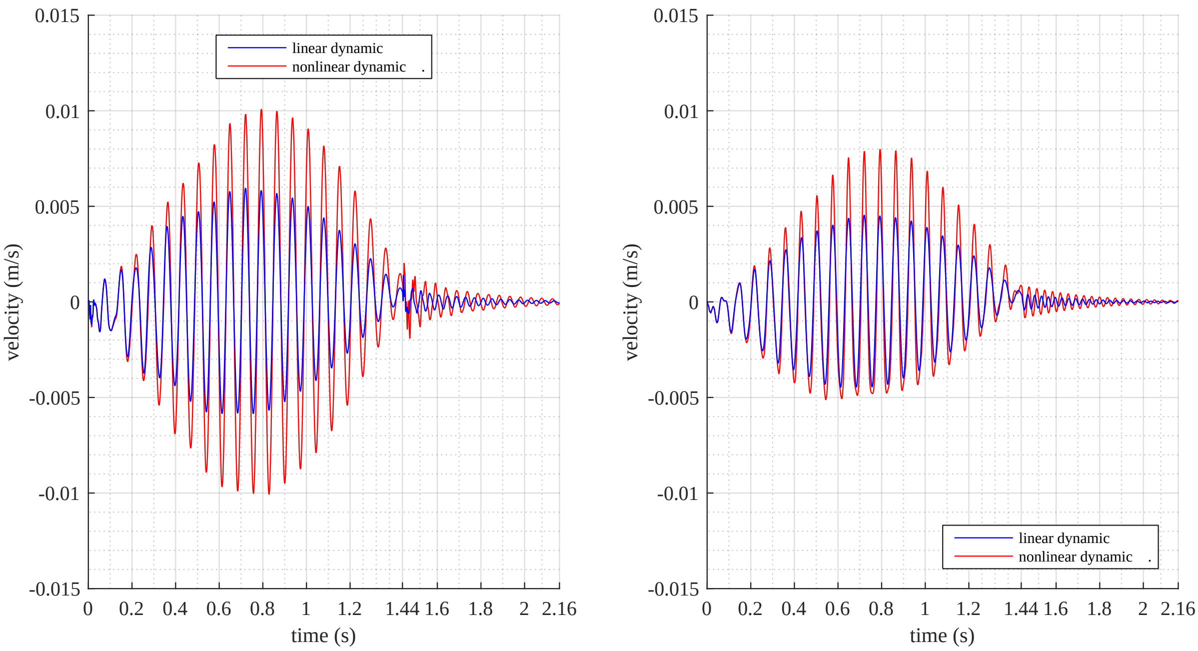

Figure 10: Dynamic responses of velocity obtained from: (a) PSS midspan, (b) *Euler-Bernoulli* midspan

Despite the limitations of both models and the lack of refinement in the mesh, the simulations were able to represent the expected responses for the two cases. This indicates an evolution of the ABXDNL routines in order to capture nonlinear dynamic effects in two-dimensional problems by damage mechanics and plasticity theory. Further investigations with improved models, especially with more complex elements, as well with different forms of irregularities, reinforcement distribution and different external actions are suggestion for future researches.

Acknowledgements

The first author would like to gratefully and sincerely thank all the other authors, teachers and staff of PPGMNE/UFPR and, also, acknowledge the financial support provided by CAPES.

REFERENCES

Abeche, T.D.O., Machado, R.D., Beghetto, F.L.M. & de Souza, L.A.F., 2015. "Computational modeling of vehicle-irregularity-bridge dynamic interaction by damage mechanics". In S. Idelsohn, V. Sonzogni, A. Coutinho, M. Cruchaga, A. Lew & M. Cerrolaza, eds., *1st Pan-American Congress on Computational Mechanics (PANACM 2015) in conjunction with the XI Argentine Congress on Computational Mechanics (MECOM 2015)*. Barcelona, Spain: International Center for Numerical Methods in Engineering (CIMNE), Buenos Aires, Argentina, Vol. 1, pp. 485–496.

Abeche, T.O., Dalledone Machado, R., Abdalla Filho, J.E., Beghetto, F.L.M. & de Souza, L.A.F., 2016. "Damage effects from dynamic interaction between vehicles, irregularities and railway bridges in the nonlinear dynamic response of structures". In J. Pombo, ed., *Third International Conference on Railway Technology: Research, Development and Maintenance (Railways 2016)*. Stirlingshire, Scotland: Civil-Comp Press, Cagliari, Sardinia, Italy, Vol. 1, pp. 1–23.

Bathe, K.J., 1996. *Finite Element Procedures*. Prentice-Hall.

Beghetto, F.L.M. & Abdalla Filho, J.E., 2010. "Modeling the dynamic response of a railway bridge and vehicle system". In B.H.V. Topping, J.M. Adam, F.J. Pallarés, R. Bru & M.L. Romero, eds., *Tenth International Conference on Computational Structures Technology*. Stirlingshire, UK: Civil-Comp Press, 23.

Jacob, B.P. & Ebecken, N.F.F., 1994. "An optimized implementation of the newmark/newton-raphson algorithm for the time integration of non-linear problems". *Communications in Numerical Methods in Engineering*, Vol. 10, No. 12, pp. 983–992.

Lemaitre, J. & Chaboche, J., 1985. "Mécanique des matériaux solides, dunod, paris.(mechanics of solid materials)". Berlin: Springer Verlag.

Lemaitre, J. & Desmorat, R., 2005. *Engineering damage mechanics: ductile, creep, fatigue and brittle failures*. Springer Science & Business Media.

Machado, R.D., 1983. *Análise dinâmica não-linear de sistemas rígido-flexíveis*. Master's thesis, Instituto Alberto Luiz Coimbra de Pós-Graduação e Pesquisa de Engenharia (COPPE), Universidade Federal do Rio de Janeiro (UFRJ), Rio de Janeiro.

Mazars, J., 1984. *Application de la mécanique de l'endommagement au comportement non linéaire et à la rupture du béton de structure*. Ph.D. thesis, Université Paris 6, Paris.

Pituba, J. & Proença, S., 2005. "Estudo e aplicação de modelos constitutivos para o concreto fundamentados na mecânica do dano contínuo". *Cadernos de Engenharia de Estruturas*, Vol. 7, No. 23, pp. 33–60.

Pituba, J.J.d.C., 1998. *Estudo e aplicação de modelos constitutivos para o concreto fundamentados na mecânica do dano contínuo*. Ph.D. thesis, Escola de Engenharia de São Carlos, Universidade de São Paulo, São Carlos.

Rabotnov, Y.N., Leckie, F. & Prager, W., 1970. "Creep problems in structural members". *Journal of Applied Mechanics*, Vol. 37, p. 249.